Reference Measurement of Roundwood by Fringe Projection

Christian Keck

René Schödel

Abstract

The metrological verification of log scanners requires logs with accurately known dimensions as test objects. The measurement of the lengths and diameters must be traceable back to the SI (International System of Units) unit of length. The results have to be reported with the corresponding measurement uncertainties. The uncertainties are required to be 5 to 10 times lower than the corresponding maximum permissible errors allowed for the log scanner under test. This article presents a procedure for the reference measurement of logs using an off-the-shelf fringe projection system along with uncertainty budgets for the measured dimensions. The length and diameters are determined from the highly resolved mesh obtained by fringe projection using techniques from computational geometry and coordinate metrology. Corrections are applied to the length and diameter values to remove the systematic effect caused by scattering of projected light below the partially transparent log surface. The influence of the fringe projection system on the measured dimensions is determined by measurements of calibrated artifacts, which also provide the traceability back to the SI unit of length. The measurement is illustrated by the example of a log with a length of 2 m and a diameter of 280 mm. The corresponding uncertainty budgets, confirmed by repeat measurements, result in expanded uncertainties (confidence interval 95**%**) of 6 mm and 0.13 mm for length and diameter, respectively. These low values qualify the fringe projection measurement along with accompanying evaluation procedure to provide logs as reference objects for the verification of log scanners.

Log scanners in sawmill conveyor lines measure lengths and diameters of roundwood by laser triangulation, with light curtains, or by ultrasound. As the diameters and lengths serve as measures for transactions of timber, among other purposes (Fonseca 2005), suppliers and sawmills expect log scanners to measure logs with adequate accuracies and high throughput under all circumstances.

As any measuring instrument brought into use, a log scanner requires verification by test measurements. Reference objects are placed on the conveyor and pass the log scanner under test. The measured lengths and diameters are compared with the values known for the reference objects. For a successful verification, the deviations of all measured values from their corresponding reference values must not exceed the permissible limits.

In order to improve the verification of log scanners, stakeholders in Germany have agreed to use logs taken as sample from the intake of sawmills, as they can be employed to obtain information on the capabilities of a scanner to cope with the natural shapes and surfaces of roundwood. They replace pipes made from cardboard, plastic, or metallic materials, which are frequent but poor choices as standards, as they can be used only to test the sensors installed in log scanners.

Before a log can be used as a reference object for verification, it is essential to measure its length and diameter with the highest possible accuracy that is justifiable in terms of effort and expense. The length and diameter are to be reported with their uncertainties, which characterize ''the dispersion of the quantity values'' (VIM, Joint Committee for Guides in Metrology 2012). Moreover, the measurements have to be traceable back to the SI (International System of Units) unit of length.

Log scanners in Germany are required to measure lengths up to 5 m with a maximum permissible error MPE_L of 50 mm. For diameters between 100 and 1,000 mm, the target for the maximum permissible error MPE_D is 10 mm (these limits are meant as examples). Good measurement practice requires the expanded (confidence interval 95%) measurement uncertainties U_L and U_D for reference lengths and diameters to be significantly lower than the corresponding maximum permissible errors MPE_L and MPE_D. OIML Guide G19 (International Organization of Legal Metrology 2017) recommends measurement uncertainties that are at

least 5 times or, better, 10 times lower than the corresponding maximum permissible errors. A reference measurement must therefore measure lengths and diameters with an uncertainty of 10 mm and 2 mm, respectively, or less.

The reference measurement requires a measuring system for stand-alone operation that is able to acquire the entire surface of a log with sufficient detail and adequate accuracy. The system should be able to be used in changing locations and not be dependent on a conveyor. The throughput required for log scanner verification is a few logs per day. In order to limit the system and development costs to a reasonable level, preference is given to an off-the-shelf system with evaluation software specially designed for the evaluation of point clouds.

Fringe projection and laser triangulation are the first choices, as they offer high accuracy along with high lateral resolution (Siekanski et al. 2019; see also the "Methodology" section). Fringe projection systems for measuring large objects with differing technical capabilities are available from several manufacturers. Laser triangulation systems measure points or lines and require extra sensors for the measurement in three dimensions (Siekanski et al. 2019 and references therein). For example, one manufacturer offers a system (Zeiss T-Scan; Carl Zeiss Optotechnik GmbH, Neubeuern, Germany) that is combination of a handheld triangulation sensor and a camera that tracks the spatial position and orientation of the triangulation sensor.

The lateral surface of logs, especially of logs in bark, places hurdles to acquisition by fringe projection and laser triangulation systems, as it may show varying brightness and may contain deep gaps and scars. Laser triangulation is less sensitive to variations in brightness. Fringe projection systems can use different camera integration times to acquire bright and dark areas sequentially. Both fringe projection and laser triangulation systems fail to acquire areas that are shaded from the light source or from the cameras.

Structure from motion (Siekanski et al. 2019) using a hand-guided digital camera can be expected to acquire the surfaces of logs with an accuracy and a resolution of details similar to fringe projection and laser triangulation systems, as it also works with electronic cameras. Nevertheless, structure from motion cannot be used for reference measurements because this method depends heavily on the optical features present on the object surface.

Terrestrial laser scanners measure distance along a laser beam by phase difference or time of flight. Typical laser scanners offer an accuracy of 3 to 10 mm at a distance of 10 m. The resolution of details on the log surface is determined by the beam diameter and lies in the order of a few mm (Luhmann et al. 2014). Terrestrial laser scanners do not meet the requirements for reference measurements.

Wood fibers with their thin, partially transparent walls and their interiors filled with air or water, cause incident light to be scattered below the surface (Kienle et al. 2008). Points are falsely recorded below the surface, causing systematic probing deviations orthogonal to the surface, which in turn reduce the measured lengths and diameters.

The preparation of an uncertainty budget requires a detailed model of measurement that considers all significant influences that affect the measurement (GUM, Joint Committee for Guides in Metrology 2008). The deviations of area-measuring instruments such as fringe projection and

laser triangulation systems can be split into probing and dimensional deviations, as demonstrated by the VDI 2634 Part 3 (Verein Deutscher Ingenieure 2008) acceptance test using calibrated spheres. Other important influences on the reference measurements can be the surface of the log, the swelling and shrinking of the log due to changes in moisture content and thermal expansion (Glass and Zelinka 2010), and the bending of the log under its own weight (Köning et al. 2009).

Methodology

Definition of length and diameter

The reference measurement addresses log scanners that capture the lateral surface of a log from all directions. The length is defined as the distance between two parallel planes at the ends of a log that encompass the crosscuts entirely and are at right angles to the longitudinal axis. The midpoint diameter is defined by the smallest minimum enclosing rectangle that is found in a section of specified length L_M around the midpoint and is aligned perpendicular to the longitudinal axis. The edges of the rectangle form a pair of diameters that together describe the diameter and the ovality in the middle of the log. This definition of the midpoint diameter requires no specification of the probing directions in which the diameters are measured.

Measurement procedure

The log is acquired using a fringe projection system. At the beginning of the measurement, the log is placed on two supports to make most parts of the surface accessible to the system, as shown in Figure 1. To minimize bending under its own weight, the log is placed symmetrically on its Bessel points.

The acquisition of the log follows standard procedures that may vary between fringe projection systems and produces a three-dimensional image of the log surface in the form of a triangulated mesh. The log surface is acquired by overlapping scans from different viewpoints around the log. Tie points placed on the log serve to connect

Figure 1.–Log (length 2 m, diameter 280 mm) on two supports in Bessel configuration before the start of fringe projection scanning. The scanning head of the fringe projection system containing the pattern projector and the cameras is seen on the left.

neighboring scans, enabling the fringe projection system to merge all scans into a single triangulated mesh. A prior photogrammetric calibration of the tie points improves the overall accuracy of the acquired point cloud.

The evaluation of the triangulated mesh employs a mixture of methods. Computational geometry (Freeman and Shapira 1975, O'Rourke 1998) is employed for operations on the triangular mesh, for example, to create cross sections and to find minimum enclosing rectangles, while the approximation of geometrical features by best-fit elements is frequently used in coordinate metrology (Shakarji 2012).

The segmentation of the crosscuts employs a heuristic approach that assumes the crosscuts to be mostly flat surfaces. It starts from an initial sample of mesh vertices taken from the center region of a crosscut. A least-squares best-fit plane calculated from the vertices serves as an initial estimate of the crosscut plane (Fig. 2a). This initial estimate is employed to identify the major part of the crosscut, which in turn provides an improved estimate of the crosscut plane (Fig. 2b). In the final step, the improved estimate is employed to identify the entire crosscut from which the crosscut plane can calculated (Fig. 2c).

To be a member of a crosscut, a mesh triangle has to meet two conditions. First, all three vertices have to lie within a given distance from the crosscut plane. Second, the misorientation of the triangle to the plane must lie below a given angular limit. For an improved identification of a crosscut, the permissible distance from the plane is lowered in the third and final step. All triangles that are not member of one of the crosscuts are assigned to the lateral surface except triangles close to one of the crosscuts. Thus, a clear separation of the lateral surface from the crosscuts is achieved (Fig. 2c).

The longitudinal axis is defined by the approximate cylinder calculated from the vertices on the lateral surface. A least-squares best-fit is chosen, as it guarantees stable results even in the presence of ovality and protrusions (e.g., caused by knots).

In the measurement of length, the crosscuts are probed not directly but rather via the crosscut best-fit planes. The vertices of each crosscut are projected onto the plane associated with the crosscut. The vertices closest to the midpoint after projection are used as contact points to measure the length, as shown in Figure 3.

To measure the midpoint diameter, cross sections are laid through the log (see Fig. 4) to find the smallest minimum enclosing rectangle. The convex hull and the minimum enclosing rectangle (Freeman and Shapira 1975) are determined for each of the cross sections (see Fig. 5). The minimum enclosing rectangle with the smallest sum of side lengths is selected to provide the orthogonal pair of diameters required for the measurement result.

Influences on the measurement

The following influence on the measurement have a significant effect on the reference measurement and are considered in the uncertainty budget:

- Fringe projection: Errors that remain after the photogrammetric calibration of the sensor and random noise cause deviations of the acquired points from their true positions. Another possible source of such deviations is the distribution of the scans over the log surface, including their overlap, the merging of the scans, and the postprocessing of the triangulated mesh. These deviations can be fully described by probing and dimensional deviations.
- Subsurface scattering: Wood fibers with their thin, partially transparent walls and their interiors filled with air or water cause incident light to be scattered below the surface. Points are falsely recorded below the surface, causing systematic probing deviations orthogonal to the surface that in turn reduce the measured lengths and diameters.
- Crosscuts: The crosscuts with their deviations from flatness control the positions and orientations of best-fit planes, and the positions of the contact points, which in turn influence the length measurement.

The following less significant influences are not considered in the uncertainty budgets:

- Lateral surface: The lateral surface of logs, especially of logs in bark, often contain deep gaps and scars that are not reached by the projector or are not seen by at least one
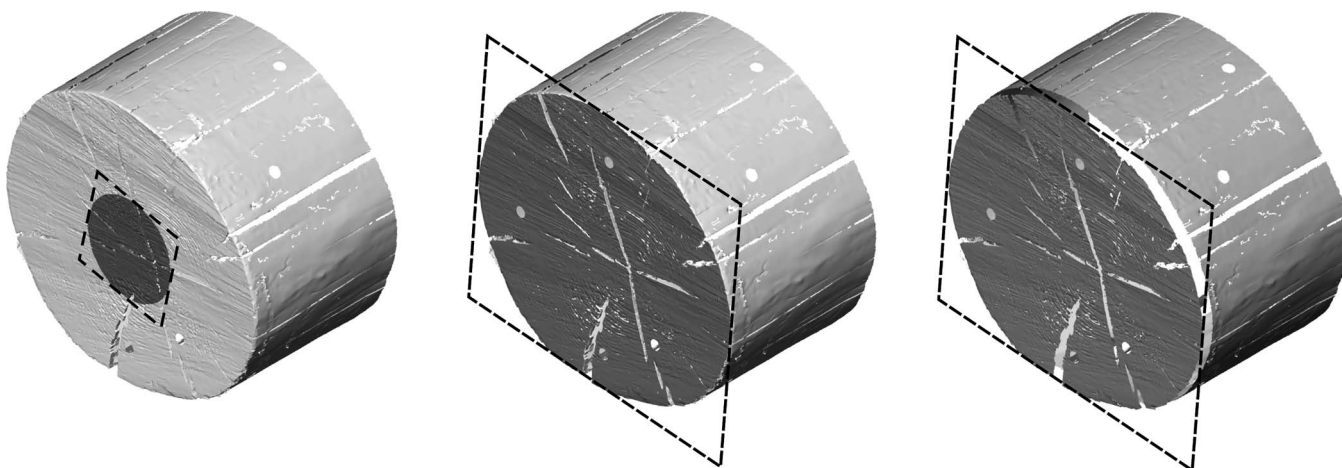

Figure 2.—Segmentation of a crosscut: (a) First estimate of the crosscut plane from an initial sample in the center. (b) Identification of most vertices in the crosscut from first estimate providing an improved estimate of the crosscut plane. (c) Segmentation of the crosscut from the lateral surface using a further improved estimate of the crosscut best-fit plane.
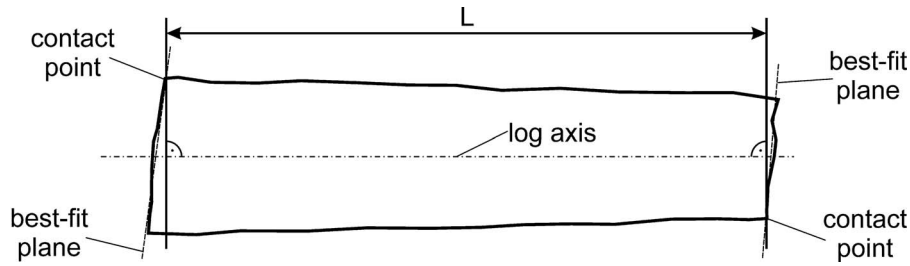
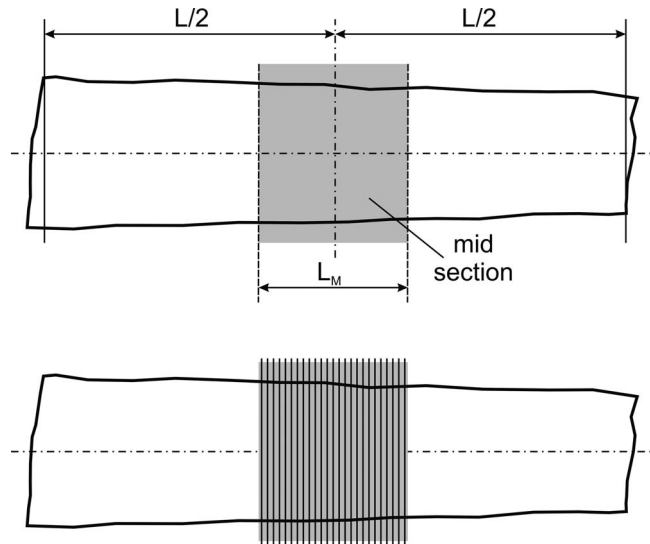Figure 3.—Measurement of the log length along the log using best-fit planes.

Figure 4.—Section in the middle of the log (length L_M) and its dissection into discrete cross sections for the determination of the midpoint diameter (schematic representation).
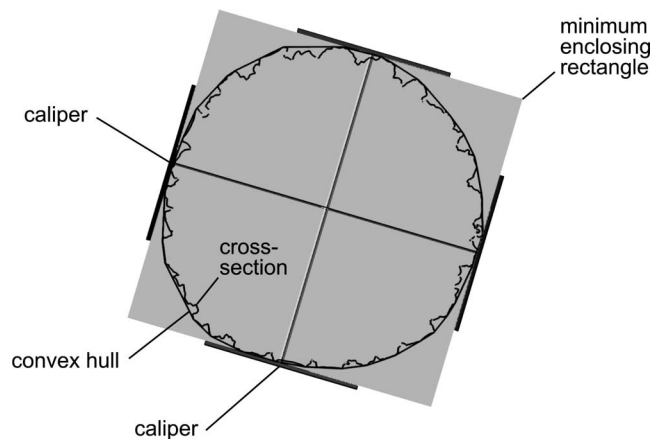

Figure 5.—Measurement of a cross section (European oak, Quercus robur, in bark, diameter 220 mm). The minimum enclosing rectangle rests on the convex hull. Its edges form two diameters perpendicular to each other, illustrated by the calipers. Valleys in the surface are ignored and do not need to be acquired by fringe projection.

of the cameras and cannot be captured. This does not affect the log axis, as the best-fit cylinder shows only minimal changes if small areas of the lateral surface are missed out or small protrusions are present. The diameter measurement is not affected by deep gaps and scars, as it depends on convex surface areas that are well captured, as shown in Figure 5.

- Crosscuts: The search range for the smallest minimum enclosing rectangle is defined by the log midpoint, which in turn is determined from the contact points on the crosscuts. The crosscuts with their deviations from flatness may cause an axial shift of the search range. In rare cases, the axial shift can affect the diameter measurement when the smallest enclosing rectangle is found close to one of the edges of the search range.
- Shrinking and swelling: Log scanners measure logs without reference to a specific moisture content or temperature. As a consequence, test measurements performed for the verification of log scanners refer to the actual lengths and diameters of the logs employed as reference. Changes in moisture and temperature that occur between the reference and test measurements will not affect the reference measurement, only the verification of log scanners. These changes are minor if the test measurements are carried out within few hours of the reference measurement since the moisture content and the temperature of logs change very slowly.
- Bending: The bending of the log under its own weight would cause the log to sag and the crosscuts to tilt. If the log is placed on supports that are close to its Bessel points of the log, the influence of bending under its own weight on the measured length and diameters can be neglected, even for the case of green logs with high specific weights and reduced elastic moduli caused by high moisture levels (Kretschmann 2010).

The probing and size errors of the fringe projection system as well as the effect of subsurface scattering have to be determined by extra measurements. The probing and size errors are determined from repeat measurements of a pair of gauge block and ring gauge. This pair simulates a log with similar dimensions and is measured in the same way as a log. The gauges provide the traceability of the measurement back to the SI unit of length.

Length uncertainty budget

The deviation ΔL of the measured length L from its true value results from the size error δ_{SLF} of the fringe projection system and from the probing errors δ_{PL1} and δ_{PL2} of the virtual contact points on the crosscuts:

$$\Delta L = \delta_{SLF} + \delta_{PL1} + \delta_{PL2} \qquad (1)$$

The error $\delta_{PL1,2}$ of a contact point on one of the crosscuts can be subdivided into the probing error $\delta_{PLF1,2}$ associated with the fringe projection, the error $\delta_{PLS1,2}$ caused by subsurface scattering, and the error $\delta_{PLC1,2}$ due to the deviation from flatness of the crosscut. Only the component acting in direction of the log axis affects the length measurement:

$$\delta_{PL1,2} = (\delta_{PLF1,2} + \delta_{PLS1,2} + \delta_{PLC1,2}) \cdot \cos\varphi_{1,2} \quad (2)$$

Since the angle $\varphi_{1,2}$ between the plane normal of a crosscut and the log axis is usually less than $\pm 15°$, $\delta_{PL1,2}$ can be approximated well by

$$\delta_{PL1,2} \approx \delta_{PLF1,2} + \delta_{PLS1,2} + \delta_{PLC1,2} \quad (3)$$

The size error δ_{SLF} from the fringe projection measurement is modeled as unknown systematic deviation in the range $\pm S_{LF}$, which is associated with an additional uncertainty u_{SLF}. The probing errors δ_{PLF1} and δ_{PLF2} coming from the fringe projection are treated as systematic deviations with unknown values in the interval $\pm P_{LF}/2$. The span P_{LF} is associated with a standard uncertainty u_{PLF}, which contributes $u_{PLF}/2$ for each of the contact points. Since the systematic effect of subsurface scattering is corrected, it is necessary to include the standard uncertainty u_{PS} of its value in the uncertainty budget. The uncertainties u_{PLC1} and u_{PLC2} associated with the deviations from flatness of the crosscuts are modeled by rectangular distributions in the ranges $\pm P_{LC1}$ and $\pm P_{LC2}$, which correspond to standard uncertainties of $P_{LC1}/\sqrt{3}$ and $P_{LC2}/\sqrt{3}$.

The above considerations result in the combined standard uncertainty u_L of the measured log length L, which is obtained by geometric addition of all contributions:

$$u_L = \sqrt{S_L^2 + u_{SL}^2 + 2 \cdot \left(\frac{P_{LF}}{2}\right)^2 + 2 \cdot \left(\frac{u_{PLF}}{2}\right)^2 + 2 \cdot u_{PS}^2 + \frac{P_{LC1}^2}{3} + \frac{P_{LC2}^2}{3}} \quad (4)$$

Uncertainty budget for a single diameter

The deviation ΔD of a single diameter D from its true value is divided into the size error δ_{SDF} caused by fringe projection and the probing errors δ_{PD1} and δ_{PD2} acting on the opposite sides of the log:

$$\Delta D = \delta_{SDF} + \delta_{PD1} + \delta_{PD2} \quad (5)$$

The probing error $\delta_{PD1,2}$ are split up into the probing error $\delta_{PDF1,2}$ associated with the fringe projection and the probing error $\delta_{PDS1,2}$ caused by subsurface scattering, respectively:

$$\Delta D = \delta_{SDF} + \delta_{PDF1} + \delta_{PDS1} + \delta_{PDF2} + \delta_{PDS2} \quad (6)$$

The contributions to the uncertainty of a single diameter are treated in a similar way to the uncertainty of the log length. Accordingly, the size error δ_{SDF} is modeled as unknown systematic deviation in the range $\pm S_{DF}$, which is associated with a standard uncertainty u_{SDF}. Again, the probing errors $\delta_{PDF1,2}$ from the fringe projection are modeled as systematic deviations of unknown value in the range $\pm P_{DF}/2$ accompanied by an additional standard uncertainty $u_{PDF}/2$. As the systematic effect of subsurface scattering is also corrected for here, the standard uncertainty

u_{PS} of the correction has to be included into the uncertainty budget.

The combined standard measurement uncertainty u_D of the diameter results from the geometrical addition of all contributions to the standard uncertainty:

$$u_D = \sqrt{S_{DF}^2 + u_{SDF}^2 + 2 \cdot \left(\frac{P_{DF}}{2}\right)^2 + 2 \cdot \left(\frac{u_{PDF}}{2}\right)^2 + 2 \cdot u_{PS}^2} \quad (7)$$

Results

Sample measurement

The measurement process as a whole is demonstrated by the example of the log shown in Figure 1. The log had been stored indoors at a temperature of $20°C \pm 1°C$ for 3 months. The log had a density of 454 kg/m^3, indicating that its moisture content had reached the equilibrium level for indoors.

The log is acquired using an ATOS III MV 1000 stereo fringe projection system (GOM GmbH, Braunschweig, Germany; scanning field 1,000 by 750 mm, maximum permissible error 0.1 mm according to VDI 2634 Part 3 for a distance of 550 mm and lateral resolution of 0.3 mm; ATOS 2017 software with custom extensions written in Python) and a single-lens reflex (SLR) digital camera (working distance 1.4 m, focal length 24 mm, aperture f/16) as accessory. The photogrammetric calibration required for a precise recording of the surface points calibration is obtained from images of a calibrated planar artifact taken by the cameras of the fringe projection sensor from multiple viewpoints followed by a bundle adjustment.

About 60 circular markers (5 mm in diameter) scattered across the log surface serve as tie points. The circular markers are calibrated using two scale bars with a length of 2 m from a series of approximately 40 images taken with the SLR camera. The capturing of the log surface with the fringe projection sensor required 25 overlapping scans. Three different integration times (T, $3T$, and $9T$) were used to avoid overexposure in bright surface areas and to capture dark areas well.

The meshes recorded on the lateral surface and on the crosscuts are shown in Figure 6. The deviation from flatness of the left crosscut ranges from -2.1 mm (valley) to $+1.9$ mm (peak), while the deviation of the right crosscut ranges from -4.5 mm to $+3.5$ mm. The normal vectors of the best-fit planes show misorientations of $1.1°$ and $1.9°$ from the log axis. The measured distance between the contact points on the crosscuts amounts to 2,017.133 mm. To correct for subsurface scattering, as discussed below, the amount of 2 by 80 μm is added to the measured value, resulting in a log length of 2,017.3 mm.

Figure 7 illustrates the measurement of the log diameter. The section around the midpoint has a length of 300 mm. An interval of 0.5 mm between the cross sections is chosen to achieve an accuracy that is superior to the log scanner under examination. The minimum enclosing rectangle is found 76.5 mm from the midpoint, with side lengths of 269.251 and 290.311 mm. Again, the effect of 2 by 80 μm subsurface scattering is corrected, resulting in diameters of 269.4 and 290.5 mm.

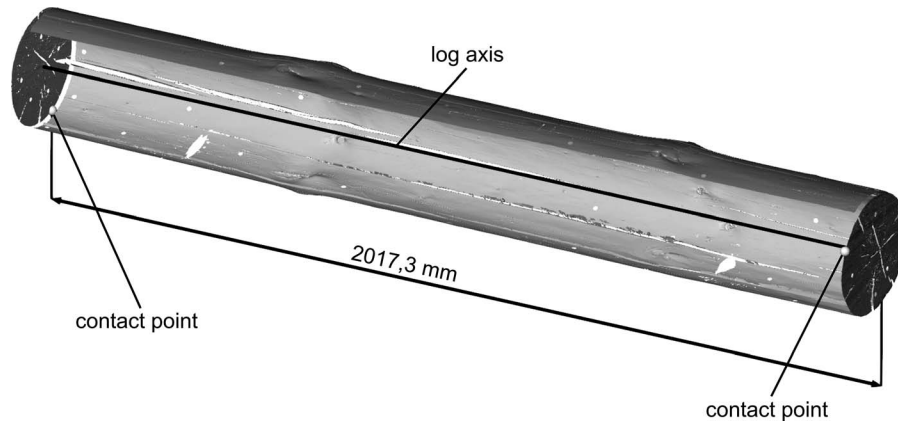The acquisition requires approximately 2 hours for the example, which includes the setup of the log on the

KECK AND SCHÖDEL

Figure 6.—Measurement of the log length. The lateral surface is partly cut away to expose the log axis.

supports, the distribution and photogrammetric calibration of the circular markers across the log surface, and the scans. The determination of the length from the acquired triangulated mesh requires a few minutes. The extraction of the diameter pair includes computing-intensive steps and requires, in the current implementation, approximately 1 hour and leaves room for improvement. The setup of the fringe projection system in a new location requires 3 hours.

Determination of the size and probing errors

The size deviation S_{LF} for the length is determined from the deviation of the measured distance between the end faces from the calibrated length of a rod in 10 repeated measurements, as summarized in Table 1. The faces of the rod (20 by 20 mm, deviation from flatness ± 5 μm) are spray coated with titanium white (coating thickness 6 to 10 μm, Palousek et al. 2015). The uncertainty budget for S_{LF} includes the variation of the measurements, the rod length calibration, and the correction of the thermal expansion. The span P_{LF} is determined from the 10 repeat recordings on a single face of the same 2-m rod as above. The best estimate

of the probing deviation P_{LF} is calculated from the mean value of the individual spans (see Table 2). Its standard uncertainty u_{PLF} comprises the variation observed in the measurements as well as the deviations from flatness and the thickness variation of the spray coating.

The size and probing errors for the measurement of diameters are determined from repeat measurements of a ring gauge made from an aluminum alloy with a diameter of 250 mm. A gray anodization provides the ring with an optically cooperative surface without reflections and glare. In each of the 10 repeat measurements, a least-squares best-fit cylinder is associated with the points acquired on the ring surface. The size error S_{DF} is determined as the mean deviation of the diameter of the best-fit cylinders from the calibrated diameter of the ring, as summarized in Table 3. Its uncertainty u_{SDF} is dominated by the observed variation of the measurements and the imperfect correction for the thermal expansion of the ring, while the subsurface scattering in the anodization plays a minor role. The probing error span P_{DF} is determined from the mean span of the radial deviation of the recorded points from the corresponding best-fit cylinder. Its uncertainty u_{PDF} is determined by the variation observed in the repeated measurements and the deviation of the ring from the form of an ideal cylinder, as shown in Table 4.
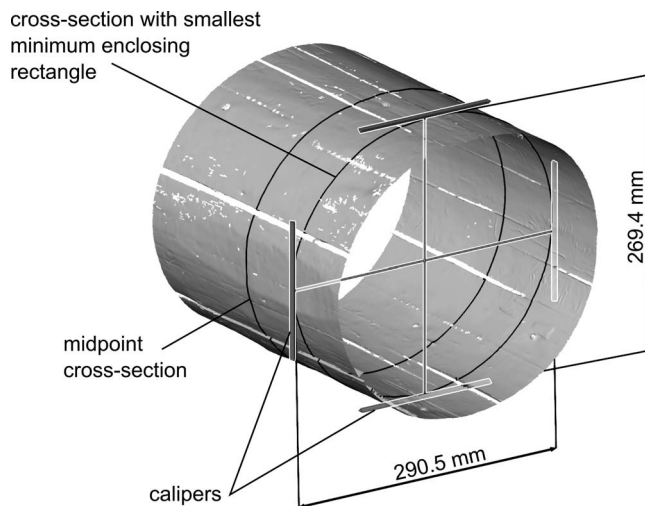
Characterization of subsurface scattering

The effect of subsurface scattering on the fringe projection is determined using the fringe projection system. Three samples from European spruce (*Picea abies*, moisture content 12% to 15%) were cut and planed to a size of 20 mm by 40 mm by 0.2 m and immersed into water for 140 hours. After removal from the bath, superfluous water was wiped off with a cloth, and the samples were left to dry in open air at room temperature for 3 hours to obtain a surface similar to green logs after debarking.

Selective spray coating with titanium white was used to fabricate optical edges. Incoming light is directly scattered in the thin coating. In uncoated areas, light penetrates the wooden surface and is scattered by the wood fibers below the surface. In a fringe projection measurement, the optical edges turn into geometrical steps whose height directly corresponds to the penetration depth of the projected patterns.

Figure 7.—Measurement of the midpoint diameter using minimum enclosing rectangles.

Table 1.—Determination of the size deviation S_{LF} *and its uncertainty* u_{SLF} *for lengths around 2 m from 10 repeated measurements of a gauge block made from steel.*

Measurements and evaluation	Value (μm)
Size deviation S_{LF}: mean value from repeated measurements after correction for thermal expansion and spray coating thickness	+6.1
Sample variation: standard deviation of repeated measurements	47.0
Standard uncertainty associated with sample variation: standard deviation in combination with an expansion factor of 1.06 for n = 10 − 1 = 9 degrees of freedom	49.8
Uncertainty budget	**Uncertainty (μm)**
Sample variation: standard uncertainty (see above)	49.8
Calibration: standard uncertainty	25.5
Thermal expansion after correction by temperature measurements: standard uncertainty (temperatures between 19°C and 21°C, maximum deviation ±3 K of the measured temperature from the true temperature including thermal inhomogeneities along the gauge, thermal expansion coefficient $(11.5 \pm 1.0 \cdot 10^{-6})$ K^{-1})	40.7
Standard uncertainty u_{SLF} (geometrical sum)	69.2

Table 2.—Determination of the probing deviation span P_{LF} *and its uncertainty* u_{PLF} *for length measurements from 10 repeated measurements of an end face of a gauge block.*

Measurements and evaluation	Value (μm)
Probing deviation span P_{LF}: mean span from repeated measurements	11.0
Sample variation: standard deviation of spans in repeated measurements	3.4
Standard uncertainty associated with sample variation: standard deviation in combination with an expansion factor of 1.06 for n = 10 − 1 = 9 degrees of freedom	3.6
Uncertainty budget	**Uncertainty (μm)**
Sample variation: standard uncertainty (see above)	3.6
Deviation from flatness: rectangular distribution within range ±5.0 μm	2.9
Irregularity of spray coating: rectangular distribution within range ±2.0 μm	1.2
Standard uncertainty u_{PLF} (geometrical sum)	4.8

Table 3.—Determination of the size deviation S_{DF} *and its uncertainty* u_{SDF} *for diameters around 250 mm from 10 repeated measurements of an aluminum ring gauge with anodized surface.*

Measurements and evaluation	Value (μm)
Size deviation S_{DF}: mean value from repeated measurements after correction of thermal expansion and anodization thickness	−20.0
Sample variation: standard deviation of repeated measurements	14.0
Standard uncertainty associated with sample variation: standard deviation in combination with an expansion factor of 1.06 for n = 10 − 1 = 9 degrees of freedom	14.8
Uncertainty budget	**Uncertainty (μm)**
Sample variation: standard uncertainty (see above)	14.8
Diameter calibration: standard uncertainty	1.0
Thermal expansion after correction by temperature measurements: standard uncertainty (temperatures between 19°C and 21°C, maximum deviation ±3 K of the measured temperature from the true temperature including thermal inhomogeneities along the gauge, thermal expansion coefficient $(23.5 \pm 1.0 \cdot 10^{-6})$ K^{-1}	10.0
Anodization thickness: Standard uncertainty	5.0
Standard uncertainty u_{SDF} (geometrical sum)	18.6

In 12 measurements, step heights between 50 and 130 μm were observed with a mean value of 88 μm and a standard deviation of 31 μm. Considering the thickness of the titanium white coating (6 to 10 μm), the step height corresponds to a systematic probing deviation P_S of 80 μm with a standard uncertainty u_{PS} of 33 μm.

Uncertainty budget for the example measurements

The uncertainty budgets for the measurement of the log length and the diameter are demonstrated by means of the example from Figure 1. In the uncertainty budget for the length shown in Table 5, the contact points on the crosscuts with their uncertainties $u_{PCL1,2}$ are by far the dominant contributors, followed by the fringe projection dimensional deviation and the probing deviation caused by subsurface scattering. The expanded measurement uncertainty U_L (95% coverage interval) of the length reaches a value of almost 5.6 mm. This value indicates that the reference measurement of length is still suitable for the verification of log scanners with an MPE$_L$ of 50 mm in length measurement.

The uncertainty budget for a single diameter is shown in Table 6. Here the influence of the probing deviations due to

Table 4: Determination of the probing deviation span P_{DF} *and its uncertainty* u_{PDF} *for cylinders with diameters around 250 mm by 10 repeated measurements of an aluminum ring gauge with anodized surface.*

Measurements and evaluation	Value (μm)
Probing deviation span P_{LF}: mean span from repeated measurements	44.2
Sample standard deviation in mm	8.3
Standard uncertainty associated with sample variation: standard deviation in combination with an expansion factor of 1.06 for n = 10 − 1 = 9 of degrees of freedom.	8.8
Uncertainty budget	Uncertainty (μm)
Sample variation: standard uncertainty	8.8
Form: rectangular distribution in range $\pm$ 27.7 μm/2	8.0
Calibration of form: standard uncertainty	1.0
Standard uncertainty u_{PDF} (geometrical sum)	11.9

the fringe projection system and to subsurface scattering dominate the uncertainty budget, while the size deviation has a weaker influence. The expanded uncertainty U_D for a single diameter amounts to 128 μm, which is significantly lower than the expanded uncertainty U_D of 2 mm required for verification of diameter measurements with an MPE$_D$ of 10 mm.

Verification of the sample measurement

In order to verify the sample measurement, 15 repeated measurements were performed within a working week. Since the humidity and the temperature in the room were kept stable, only minor dimensional changes were expected. At the beginning of each measurement, a new set of circular markers was distributed on the log surface to be calibrated using the SLR camera. The calibration of the fringe projection sensor was performed once before the start of the series.

The measurement results are summarized in Table 7. Measured lengths and diameters are in good agreement. The standard deviation of 55 μm of the measured diameters agrees well with the predicted measurement uncertainty u_D of 64 μm (see Table 6). The standard deviation of the measured lengths is much lower than the predicted standard uncertainty of 2.8 mm (see Table 5). The sample standard deviation of 55 μm is comparable in size with the standard

uncertainty of 84 μm, which is obtained when the contribution from the crosscuts are ignored, and supports the approach taken for the uncertainty budget.

Discussion

The high accuracy of the fringe projection measurement is achieved by measuring the log at rest and making use of many available options of the fringe projection system, especially to acquire images on the log surface with three different camera integration times and the photogrammetric calibration of the tie points on the log surface, which improves the overall accuracy of the acquired triangulated mesh. The systematic influence of subsurface scattering reaches the same order of magnitude as the influences coming from the fringe projection system and must be corrected, especially in the diameter measurement. In the length measurement, the crosscuts with their deviations from flatness dominate the measurement uncertainty.

General experience shows that dimensional deviations δ_{SLF} and δ_{SDF} caused by the fringe projection system and the corresponding contributions to the uncertainty budget grow with increasing log size, while the probing deviations δ_{PLF} and δ_{PDF} and the corresponding uncertainties are expected to remain constant.

Other fringe projection system may produce slightly different measurement results with different uncertainties

Table 5.—Uncertainty budget for the measurement of the log length L *of approximately 2 m.*

	Influence	Characteristic	Uncertainty (μm)
Size deviations			
S_{LF}	Size error due to fringe projection	Systematic deviation without correction (see Table 1)	6
u_{SLF}	Size error due to fringe projection	Standard uncertainty (see Table 1)	69
Probing error for contact point on left crosscut			
$P_{LF}/2$	Probing error due to fringe projection	Unknown systematic deviation without correction in the range $\pm P_{LF}/2$ (see Table 2)	7
$u_{PLF}/2$	Probing error due to fringe projection	Standard uncertainty (see Table 2)	3
u_{PS}	Probing error due to subsurface scattering	Standard uncertainty after correction of the systematic deviation	33
u_{LC1}	Deviation from flatness	Rectangular distribution in range ± 2.1 mm	1,270
Probing error for contact point on right crosscut			
$P_{LF}/2$	Probing error due to fringe projection	Systematic deviation without correction in the range $\pm P_{LF}/2$ (see Table 2)	7
$u_{PLF}/2$	Probing error due to fringe projection	Standard uncertainty (see Table 2)	3
u_{PS}	Probing error due to subsurface scattering	Standard uncertainty after correction of the systematic deviation	33
u_{LC2}	Deviation from flatness	Rectangular distribution in range ± 4.5 mm	2,598
Length measurement			
u_L	Standard uncertainty (k = 1), geometrical sum		2,893
U_L	Expanded uncertainty (k = 2, confidence interval 95%)		5,786

Table 6.—Uncertainty for the measurement of a single diameter D *of approximately 250 mm.*

Influence		Characteristic	Uncertainty (μm)
Size error			
S_{DF}	Size error due to fringe projection	Unknown systematic deviation without correction (see Table 3)	20
u_{SDF}	Size error due to fringe projection	Standard uncertainty (see Table 3)	19
Probing error for contact point on circumference			
$P_{DF}/2$	Probing error due to fringe projection	Systematic deviation without correction (see Table 3)	22
$u_{PDF}/2$	Probing error due to fringe projection	Standard uncertainty (see Table 3)	6
u_{PS}	Probing error due to volume scattering remaining after correction	Standard uncertainty	33
Probing error for contact point on opposite side of circumference			
$P_{DF}/2$	Probing error due to fringe projection	Systematic deviation without correction	22
$u_{PDF}/2$	Probing error due to fringe projection	Standard uncertainty	6
u_{PS}	Probing error due to volume scattering remaining after correction	Standard uncertainty	33
Single diameter			
u_D	Standard uncertainty (k = 1, geometrical sum)		64
U_D	Expanded uncertainty (k = 2, confidence interval 95%)		128

depending on the size of the measuring field and the measuring capabilities. Some systems may require modifications to the evaluation procedures and the uncertainty budgets if the capabilities of the evaluation software differ from the software used here.

The effect of subsurface scattering is certainly dependent on the tree species. The approach shown above is a pragmatic way that does not require any extra measuring instrument other than the fringe projection system. The measured step heights are close to the accuracy limit of fringe projection systems.

The measured lengths and diameters according to the above procedure are meant for the evaluation of log scanners that measure logs according to the same definition. They cannot be used directly for the verification of scanners that measure midpoint diameters along fixed given probing directions or measure the diameters in separate cross sections. These types of scanners are not able to find the same smallest minimum enclosing rectangle and arrive at different diameter results. In these cases, the measurement procedure has to be modified to permit the specification of the probing directions. Also, the specification of the probing directions might become another contributor to the diameter measurement uncertainty budget.

The determination of probing and size errors by additional measurements requires standards that can be manufactured with high precision and calibrated with a sufficiently low uncertainty. In particular, large ring gauges are difficult to manufacture and calibrate. This manifests itself in larger form deviations and calibration uncertainties that further increase the contribution of the size and probing deviations to the diameter uncertainty budget. The weight of such gauge rings increases quadratically with the diameter,

Table 7.—Results of the repeated measurements (mm) of the log from Figure 1.

	Length, L	Diameter, D	Diameter, $D_{90°}$
Sample mean	2,017.122	269.151	290.237
Sample median	2,017.136	269.147	290.227
Span	0.204	0.191	0.170
Standard deviation	0.055	0.055	0.057

making them difficult to handle unless lightweight materials and/or techniques are available.

Assessing the performance of the reference measurement in terms other than accuracy and throughput is difficult. The proposed uncertainty budgets along with the underlying model form a simple yet powerful tool for the accuracy assessment of the reference measurement. The black-box model, which differentiates only between dimensional and probing deviations in length and diameter measurements, is generally able to describe the metrological behavior of fringe projection and laser triangulation systems equally well. The contributions of the measuring system to the uncertainties can be determined by repeat measurements of gauges and can be adapted to different log sizes with reasonable effort.

The throughput of the measuring system is limited mainly by the high amount of labor required for the photogrammetric calibration of the tie points using the extra SLR camera and the scans of the log surface. In the course of the calibration of the tie points, images have to be manually taken from various positions, including positions high above the log. For each of the scans, the heavy (10 kg) scanning head of the fringe projection system has to be manually positioned in front of the corresponding part of the log surface. If a fringe projection system with a smaller measuring field is employed for the measurement, the number of scans and the time required for the acquisition of a log will rise drastically. The laser triangulation system mentioned in the introduction requires the operator to slowly scan the log section by section, also leading to a high amount of manual labor.

Conclusions

This article demonstrates the dimensional measurement of roundwood with high accuracy by fringe projection using an off-the-shelf measuring system. It presents measurement budgets for the measured lengths and diameters and can be swiftly adapted to logs of different sizes. The contributions of the dimensional and probing deviations to the measurement uncertainties are determined from repeat measurements of gauges that simulate the log with its geometry and require no insight into the fringe projection system. Care is

KECK AND SCHÖDEL

taken to compensate for the systematic effect of subsurface scattering on the measurement.

The measurement uncertainties derived for the log length and diameters qualify this measurement process as an accurate reference for the verification of log scanners. The primary limitation lies in the availability of calibrated gauge blocks and ring gauges with lengths and diameters like the logs that are to be measured. Without suitable gauges, it is not possible to state measurement uncertainties, which are indispensable in the metrological verification of measuring systems. The low throughput of a few logs per day is not expected to be a limitation in the verification of log scanners. The approach can also be extended to provide reference values for the taper or sweep, both of which also rely on the measurement of cross sections. Also, the volume of logs can be calculated accurately from the triangulated mesh.

Fringe projection and laser triangulation systems have a large potential in the verification of other measuring systems in the sawmill industry since they permit the acquisition of the entire surface of a large object in the form of a single triangulated mesh with high accuracy and resolution. The main prerequisite is the availability of suitable geometrical standards that allow for the proper determination of the dimensional and probing deviations of the measuring system. The low throughput would be an obstacle only if a larger sample of reference objects were required.

Literature Cited

Fonseca, M. 2005. Measurement of Roundwood: Methodologies and Conversion Ratios. CABI Publishing, Cambridge, UK.

Freeman, H. and R. Shapira. 1975. Determining the minimum-area encasing rectangle for an arbitrary closed curve. *Commun. ACM* 18(7):409–413.

Glass, S. and S. Zelinka. 2010. Moisture relations and physical properties of wood. *In:* Wood Handbook —Wood as an Engineering Material. Centennial Edition. General Technical Report FPL-GTR-190. R. J. Ross (Ed.). U.S. Forest Service, Forest Products Laboratory, Madison, Wisconsin. pp. 4-1–4-19.

International Organization of Legal Metrology. 2017. The role of measurement uncertainty in conformity assessment decisions in legal metrology. OIML G19. International Organization of Legal Metrology, Paris, France.

Joint Committee for Guides in Metrology. 2008. Evaluation of measurement data—Guide to the expression of uncertainty in measurement (GUM). JCGM 100. Joint Committee for Guides in Metrology, Sevres, France.

Joint Committee for Guides in Metrology. 2012. International vocabulary of metrology—Basic and general concepts and associated terms (VIM). JCGM 200. Joint Committee for Guides in Metrology, Sevres, France.

Kienle, A., C. D'Andrea, F. Foschum, P. Taroni, and A. Pifferi. 2008. Light propagation in dry and wet softwood. *Optics Express* 16:9895–9906.

Köning, R., B. Przebierala, C. Weichert, J. Flügge, and H. Bosse. 2009. A revised treatment of the influence of the sample support on the measurement of line scales and the consequences for its use to disseminate the unit of length. *Metrologia* 46(3):187–195.

Kretschmann, D. E. 2010. Mechanical properties of wood. *In:* Wood Handbook—Wood as an Engineering Material. Centennial Edition. General Technical Report FPL-GTR-190. R. J. Ross (Ed.). U.S. Forest Service, Forest Products Laboratory, Madison, Wisconsin. pp. 5-1–5-46.

Luhmann, T., S. Robson, S. Kyle, and J. Boehm. 2014. Close-Range Photogrammetry and 3D Imaging. De Gruyter, Berlin, Germany.

O'Rourke, J. 1998. Computational Geometry in C. Cambridge University Press, Cambridge, UK.

Palousek, D., M. Omasta, D. Koutny, J. Bednar, T. Koutecky, and F. Dokoupil. 2015. Effect of matte coating on 3D optical measurement accuracy. *Optical Mater.* 40:1–9.

Sharkarji, C. M. 2012. Coordinate measuring system algorithms and filters. *In:* Coordinate Measuring Machines and Systems. R. J. Hocken, and P. H. Pereira (Eds.). CRC Press, Boca Raton, FL. pp. 153–182.

Siekanski, P., K. Magda, K. Malowany, J. Rutkiewicz, A. Styk, J. Krzesłowski, T. Kowaluk, and A. Zagórski. 2019. On-line laser triangulation scanner for wood logs surface geometry measurement. *Sensors* 19:1074.

Verein Deutscher Ingenieure. 2008. Optical 3D-measuring systems—Multiple view systems based on area scanning. VDI 2634 Part 3. Verein Deutscher Ingenieure, Düsseldorf, Germany.